A&A 407, 769–778 (2003)
DOI: 10.1051/0004-6361:20030874

Astronomy & Astrophysics

Excitation rates for transitions in Ca XV⋆

K. M. Aggarwal and F. P. Keenan

Department of Pure and Applied Physics, The Queen's University of Belfast, Belfast BT7 1NN, Northern Ireland, UK

Received 17 March 2003 / Accepted 22 May 2003

Abstract. Collision strengths for transitions among the energetically lowest 46 fine-structure levels belonging to the $(1s^2)$ $2s^22p^2$, $2s2p^3$, $2p^4$, and $2s^22p3\ell$ configurations of Ca XV are computed, over a wide electron energy range below 300 Ryd, using the Dirac Atomic R-matrix Code (DARC) of Norrington & Grant (2003). Resonances in the threshold region have been resolved in a fine energy mesh, and excitation rates are determined over a wide electron temperature range below 10^7 K. The results are compared with those available in the literature, and the accuracy of the data is assessed.

Key words. atomic data - atomic processes

1. Introduction

In a recent paper (Aggarwal & Keenan 2002) we reported results for electron impact excitation collision strengths (Ω) for resonance transitions in Ca XV, at a few representative energies above thresholds. Similar results for excitation rate coefficients, which are determined after integrating values of Ω over a Maxwellian distribution of electron velocities, were not reported because our calculations in the threshold region were still in progress. Since then we have resolved resonances in a fine energy mesh over the entire threshold region, and hence present our results of excitation rates, in the form of effective collision strengths (Υ), for *all* transitions among the 46 fine-structure levels belonging to the $(1s^2)$ $2s^22p^2$, $2s2p^3$, $2p^4$ and $2s^22p3\ell$ configurations of Ca XV. The corresponding results for energy levels and radiative rates have already been reported in our earlier publication (Aggarwal et al 1997).

Calcium is an abundant element in the solar corona and chromosphere. Its emission lines have been observed from many ionization stages, and lines from Ca XV have particularly been useful as density diagnostics of solar flares – see, for example, Keenan et al. (1992). Additionally, its lines are also useful in laboratory and laser plasmas. Therefore, atomic data for energy levels, radiative rates, collision strengths, and rate coefficients are always in demand.

Earlier work on this ion has been performed by many workers. The prominent among these are the *R*-matrix calculations of Aggarwal (1992), and the *Distorted-Wave* (DW) results of Bhatia & Doschek (1993) and Zhang & Sampson (1996). However, the *DW* calculations have only been performed for values of Ω at a few energies *above* thresholds, from which accurate values of rate coefficients cannot be determined, because resonances in the threshold region have not been delineated. It is well established by now that the closed-channel (Feshbach) resonances considerably enhance values of rate coefficients, even at a temperature of $10^{6.6}$ K, where Ca XV has its maximum ionization abundance (Mazzotta et al 1985). Additionally, the calculations of Zhang & Sampson are limited to transitions among the lowest 20 fine-structure levels of the $(1s^2)$ $2s^22p^2$, $2s2p^3$ and $2p^4$ configurations, whereas Bhatia & Doschek have also included the additional 26 fine-structure levels among the $(1s^22s^22p)$ 3s, 3p and 3d configurations. Similarly, our earlier calculations are also confined to the lowest 20 fine-structure levels, whereas data are also required among higher levels for diagnostic studies of solar and laboratory plasmas. Moreover, in spite of including the resonances for the computation of rates, the earlier *R*-matrix calculations suffer from three major deficiencies. Firstly, calculations for Ω were restricted to partial waves with angular momentum $J \leq 14.5$. This affects the accuracy of the derived values of Ω, especially at higher energies, as has already been demonstrated in our previous paper (Aggarwal & Keenan 2002). Secondly, values of Ω were computed up to an energy of 200 Ryd only. This affects the calculations of Υ, especially at higher temperatures. Finally, the energy mesh adopted in our earlier calculations was comparatively coarse ($\Delta E \leq 0.01$ Ryd). This affects the accuracy of Υ values, particularly for the forbidden transitions for which resonances are more important. All of these restrictions were due to the computational limitations at that time. In our present work, we are extending the partial wave range up to $J = 40.5$, and the energy range up to 300 Ryd. Furthermore, to delineate resonances our present energy mesh is ≤0.002 Ryd. Therefore,

Send offprint requests to: K. M. Aggarwal,
e-mail: K.Aggarwal@qub.ac.uk

⋆ Table 3 is also (and Table 4 only) available in electronic form at the CDS via anonymous ftp to cdsarc.u-strasbg.fr (130.79.128.5) or via
http://cdsweb.u-strasbg.fr/cgi-bin/qcat?J/A+A/407/769

apart from computing our results for a larger number of transitions among the lowest 46 fine-structure levels of Ca XV, we are attempting to make a significant overall improvement over our earlier results.

2. Calculation details

For the generation of wavefunctions, we have adopted the GRASP (General-purpose Relativistic Atomic Structure Program) code of Dyall et al. (1989), which is a fully relativistic code. Additionally, configuration interaction (CI) among the above listed six configurations was also included, and results for energy levels, radiative rates and oscillator strengths for transitions in Ca XV have already been reported and discussed (Aggarwal et al 1997). In Table 1 we list our energy levels for a ready reference and also provide an index for each level for further discussion of results. The experimentally compiled energies of Sugar & Corliss (1985) are also listed in this table. It may be noted that the experimental energies are not available for all the levels, but the agreement between the common experimental and theoretical level energies is within 2%, which is highly satisfactory. However, our $2s2p^3\ {}^5S^o_2$ level energy is lower than the experimental one by 4%.

For computations of Ω, we have employed the fully relativistic Dirac Atomic *R*- matrix Code (DARC) of Norrington & Grant (2003). This program includes the relativistic effects in a systematic way, in both the target description and the scattering model. However, because of the inclusion of fine-structure in the definition of channel coupling, the matrix size of the Hamiltonian increases substantially, making the calculations computationally quite expensive. The *R*- matrix boundary radius has been taken to be 3.0 au, and 23 continuum orbitals have been included for each channel angular momentum, for the expansion of the wavefunction. This allows us to compute Ω up to an energy of 300 Ryd, more than sufficient for the calculation of accurate excitation and de-excitation rate coefficients for temperatures up to 10^7 K. The maximum number of channels for a partial wave is 178, and the corresponding size of the Hamiltonian matrix is 4106. In order to obtain converged Ω at all energies (especially the higher ones) and for all transitions (particularly the allowed ones), we have included the contribution of all partial waves with angular momentum $J \leq 40.5$. Although Ω for most of the transitions have converged due to the inclusion of such a large range of partial waves, there are some allowed transitions for which even this large range is not sufficient for convergence. Therefore, to take account of higher neglected partial waves, a top-up based on the Coulomb-Bethe approximation for allowed transitions, and geometric series for other remaining transitions has been included.

Since comparison of our collision strengths with the other available data of Aggarwal (1992), Bhatia & Doschek (1993) and Zhang & Sampson (1996) has already been discussed in our previous paper (Aggarwal & Keenan 2002), we focus our attention on the results of excitation rates in the following section.

Table 1. Target levels of Ca XV and their threshold energies (in Ryd).

Index	Configuration	Level	Expt.[a]	GRASP[b]
1	$1s^22s^22p^2$	$^3P_0$	0.0000	0.0000
2	$1s^22s^22p^2$	$^3P_1$	0.1600	0.1601
3	$1s^22s^22p^2$	$^3P_2$	0.3273	0.3281
4	$1s^22s^22p^2$	$^1D_2$	0.9896	1.0138
5	$1s^22s^22p^2$	$^1S_0$	1.8009	1.7695
6	$1s^22s2p^3$	$^5S_2{}^o$	2.4985	2.3928
7	$1s^22s2p^3$	$^3D_2{}^o$	4.5261	4.5364
8	$1s^22s2p^3$	$^3D_1{}^o$	4.5344	4.5456
9	$1s^22s2p^3$	$^3D_3{}^o$	4.5585	4.5677
10	$1s^22s2p^3$	$^3P_0{}^o$	5.3011	5.3144
11	$1s^22s2p^3$	$^3P_1{}^o$	5.3112	5.3246
12	$1s^22s2p^3$	$^3P_2{}^o$	5.3369	5.3500
13	$1s^22s2p^3$	$^3S_1{}^o$	6.6423	6.7940
14	$1s^22s2p^3$	$^1D_2{}^o$	6.6497	6.7971
15	$1s^22s2p^3$	$^1P_1{}^o$	7.4211	7.5695
16	$1s^22p^4$	$^3P_2$	10.0929	10.2321
17	$1s^22p^4$	$^3P_1$	10.3326	10.4681
18	$1s^22p^4$	$^3P_0$	10.3897	10.5269
19	$1s^22p^4$	$^1D_2$	10.8915	11.1048
20	$1s^22p^4$	$^1S_0$	12.3397	12.5692
21	$1s^22s^22p3s$	$^3P_0{}^o$	.....	37.4440
22	$1s^22s^22p3s$	$^3P_1{}^o$	.....	37.4905
23	$1s^22s^22p3s$	$^3P_2{}^o$	.....	37.7821
24	$1s^22s^22p3s$	$^1P_1{}^o$	.....	37.9481
25	$1s^22s^22p3p$	$^3D_1$	.....	38.5909
26	$1s^22s^22p3p$	$^3D_2$	.....	38.8009
27	$1s^22s^22p3p$	$^1P_1$	.....	38.8099
28	$1s^22s^22p3p$	$^3D_3$	.....	39.0419
29	$1s^22s^22p3p$	$^3S_1$	.....	39.0900
30	$1s^22s^22p3p$	$^3P_0$	.....	39.1045
31	$1s^22s^22p3p$	$^3P_1$	.....	39.2720
32	$1s^22s^22p3p$	$^3P_2$	.....	39.3384
33	$1s^22s^22p3p$	$^1D_2$	.....	39.6112
34	$1s^22s^22p3d$	$^3F_2{}^o$	39.7586	39.9877
35	$1s^22s^22p3p$	$^1S_0$	.....	40.0342
36	$1s^22s^22p3d$	$^3F_3{}^o$	39.9044	40.1271
37	$1s^22s^22p3d$	$^1D_2{}^o$	.....	40.1990
38	$1s^22s^22p3d$	$^3F_4{}^o$	.....	40.3352
39	$1s^22s^22p3d$	$^3D_1{}^o$	40.0866	40.3696
40	$1s^22s^22p3d$	$^3D_2{}^o$	40.2051	40.4639
41	$1s^22s^22p3d$	$^3D_3{}^o$	40.3327	40.5833
42	$1s^22s^22p3d$	$^3P_2{}^o$	40.4147	40.6537
43	$1s^22s^22p3d$	$^3P_1{}^o$	40.4147	40.6719
44	$1s^22s^22p3d$	$^3P_0{}^o$	.....	40.6853
45	$1s^22s^22p3d$	$^1P_1{}^o$	40.7610	41.0566
46	$1s^22s^22p3d$	$^1F_3{}^o$	40.7792	41.0685

a. Sugar & Corliss (1985).
b. Aggarwal et al. (1997).

3. Excitation rates

The values of excitation $q(i, j)$ and de-excitation $q(j, i)$ rate coefficients are related to effective collision strengths (Υ) as follows:

$$q(i, j) = \frac{8.63 \times 10^{-6}}{\omega_i T_e^{1/2}} \Upsilon \exp(-E_{ij}/kT_e) \qquad \mathrm{cm^3\,s^{-1}} \qquad (1)$$

and

$$q(j, i) = \frac{8.63 \times 10^{-6}}{\omega_j T_e^{1/2}} \Upsilon \qquad \mathrm{cm^3\,s^{-1}}, \qquad (2)$$

where ω_i and ω_j are the statistical weights of the initial (i) and final (j) states, respectively, E_{ij} is the transition energy, k is Boltzmann constant, and T_e is electron temperature in K. Values of Υ are obtained after integrating the Ω data over a Maxwellian distribution of electron velocities as follows:

$$\Upsilon(T_e) = \int_0^\infty \Omega(E) \exp(-E_j/kT_e) \mathrm{d}(E_j/kT_e), \qquad (3)$$

where E_j is the electron energy with respect to the final (excited) state.

Since the threshold region is dominated by numerous resonances, Ω must be computed in a fine mesh of energy. Close to thresholds our mesh is 0.001 Ryd and is 0.002 Ryd in the remaining range. In total, values of Ω have been computed at over 21 700 energies in the threshold region below 41 Ryd. This fine energy mesh ensures to a large extent that neither a majority of resonances are missed, nor do the exceptionally high resonances have unreasonably large width. In Figs. 1–3 (a and b) we show resonances for only three transitions, namely ($2s^2 2p^2$) $^3P_0$–$^3P_1$ (1–2), $^3P_1$–$^3P_2$ (2–3), and $^1D_2$–$^1S_0$ (4–5), respectively. These are the *same* transitions for which resonances have also been shown in our earlier work (Aggarwal 1992), and hence facilitate a ready comparison, as well as provide a good idea about their density and importance. In Figs. 1a–3a the energy and Ω scale are exactly the *same* as in Figs. 1–3 of Aggarwal (1992), but Figs. 1b–3b show values of Ω in a wider energy region below 40 Ryd.

In Table 2 we compare our present (RM1) and earlier (RM2: Aggarwal 1992) results for Υ for transitions among the $1s^2 2s^2 2p^2$ ground configuration of Ca XV, at three temperatures, i.e. 10^5, 10^6, and 10^7 K. It is surprising to note differences of a factor of two for many transitions (such as: 1–5 and 3–5), and over almost the entire temperature range. Since differences between our present and the past calculations are the highest (up to a factor of four at $T_e = 10^6$ K) for the $^3P_0$–$^3P_2$ (1–3) transition, we have a closer look at the Ω values for this. In Figs. 4a,b we demonstrate its Ω values in the entire threshold region. As seen in Fig. 4a, at energies below 7 Ryd (~10^6 K), this transition has many resonances whose magnitude are considerably high compared to its background value (~0.02). The higher thresholds range also demonstrates resonances for this transition as shown in Fig. 4b, but their density and magnitude are comparatively lower. However, the magnitude of Ω at energies above thresholds are nearly the same (within 10%) in both of our calculations. Due to a coarser energy mesh adopted in our earlier calculations, as explained in Sect. 1, the

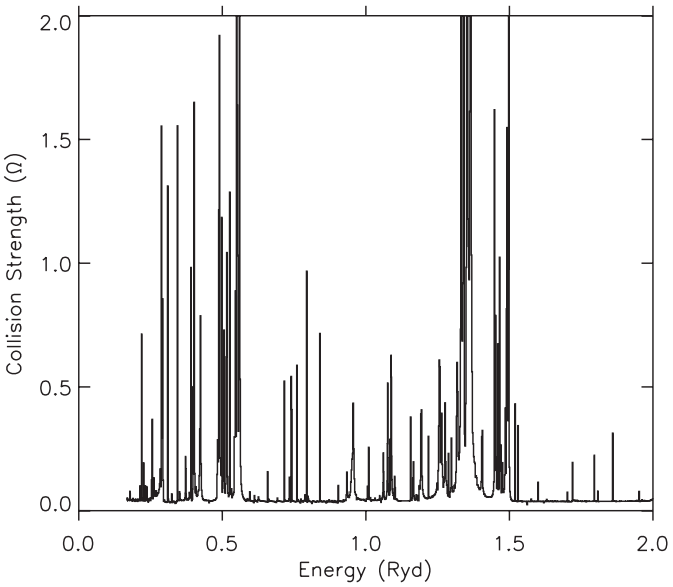

(a)

Fig. 1. Collision strengths (Ω) for the ($2s^2 2p^2$) $^3P_0$–$^3P_1$ (1–2) transition of Ca XV. **a)** Results below 2 Ryd and **b)** results in entire threshold region up to 40 Ryd.

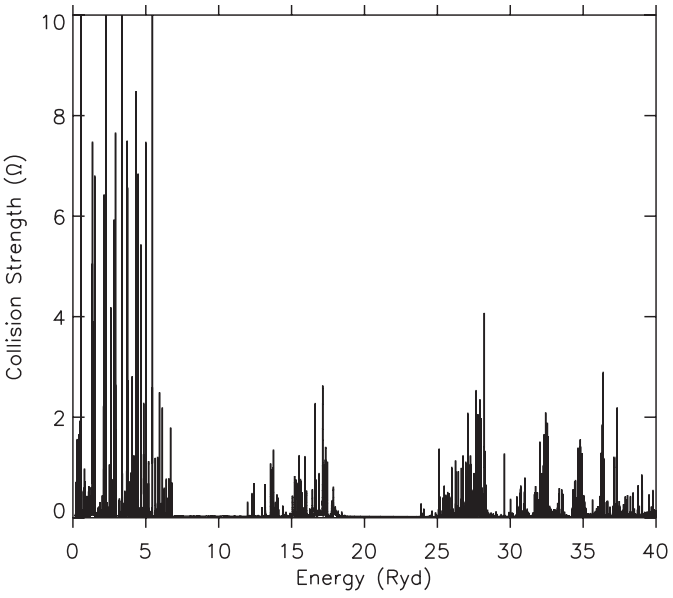

(b)

Fig. 1. Collision strengths (Ω) for the ($2s^2 2p^2$) $^3P_0$–$^3P_1$ (1–2) transition of Ca XV. **a)** Results below 2 Ryd and **b)** results in entire threshold region up to 40 Ryd.

contribution of some of these resonances has obviously been overestimated. For example, in our earlier calculations, Ω was computed at ~2900 energies in the range below the $2p^4\ ^1S_0$ threshold (~12.57 Ryd), whereas in the present calculations we have computed Ω at ~6700 energies in the same energy range. This and other improvements made in the present calculations have significantly affected the earlier values of Υ for many transitions. Some transitions have been affected more towards the lower end of the temperature range (such as 1–2), some at higher temperatures (such as 4–5), and some at all temperatures (such as 1–3 and 3–5). The transitions which have particularly

Table 2. Comparison between present (RM1) and earlier (RM2: Aggarwal 1992) results of effective collision strengths for transitions within the levels of the ($1s^2 2s^2 2p^2$) ground configuration of Ca XV. ($a \pm b \equiv a \times 10^{\pm b}$).

log T_e		5.0	5.0	6.0	6.0	7.0	7.0 K
Transition	I–J	RM1	RM2	RM1	RM2	RM1	RM2
$^3P_0$–$^3P_1$	1–2	2.387-1	1.679-1	1.258-1	1.743-1	3.885-2	3.872-2
$^3P_0$–$^3P_2$	1–3	6.914-2	1.211-1	5.799-2	2.430-1	2.780-2	5.157-2
$^3P_0$–$^1D_2$	1–4	4.855-2	4.178-2	2.573-2	2.187-2	1.225-2	7.742-3
$^3P_0$–$^1S_0$	1–5	8.017-3	1.327-2	5.628-3	7.203-3	3.231-3	1.493-3
$^3P_1$–$^3P_2$	2–3	3.911-1	5.386-1	4.647-1	8.777-1	1.372-1	1.911-1
$^3P_1$–$^1D_2$	2–4	1.665-1	1.555-1	9.944-2	9.186-2	4.981-2	3.181-2
$^3P_1$–$^1S_0$	2–5	2.269-2	3.104-2	1.822-2	1.797-2	1.041-2	4.974-3
$^3P_2$–$^1D_2$	3–4	3.926-1	3.899-1	2.455-1	3.602-1	1.102-1	1.001-1
$^3P_2$–$^1S_0$	3–5	2.339-2	4.975-2	2.262-2	3.220-2	1.462-2	9.405-3
$^1D_2$–$^1S_0$	4–5	2.023-1	2.105-1	1.052-1	9.690-2	5.912-2	4.982-2

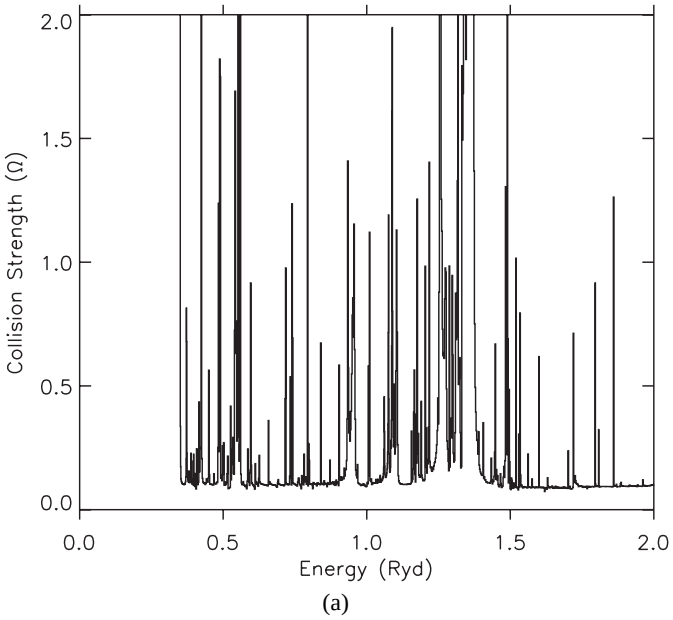

(a)

Fig. 2. Collision strengths (Ω) for the ($2s^2 2p^2$) $^3P_1$–$^3P_2$ (2–3) transition of Ca XV. **a)** Results below 2 Ryd and **b)** results in entire threshold region up to 40 Ryd.

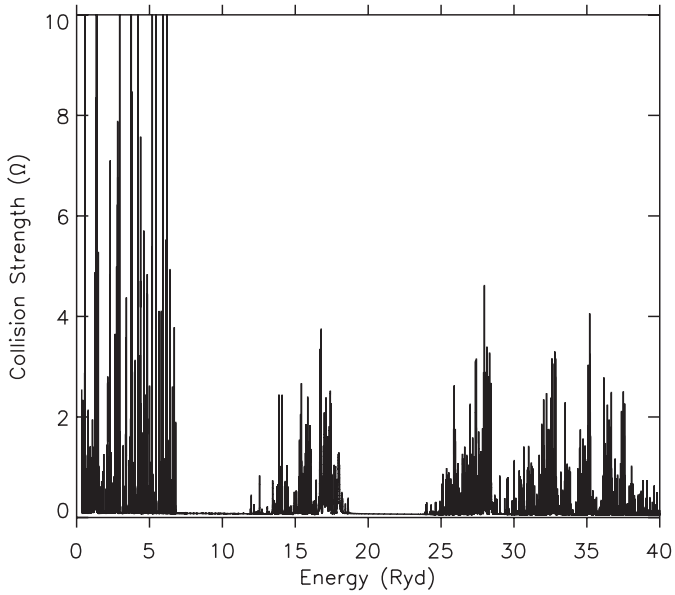

(b)

Fig. 2. Collision strengths (Ω) for the ($2s^2 2p^2$) $^3P_1$–$^3P_2$ (2–3) transition of Ca XV. **a)** Results below 2 Ryd and **b)** results in entire threshold region up to 40 Ryd.

been affected (up to an order of magnitude) are those whose upper levels belong to the $2p^4$ configuration (i.e. 16–20). This is because resonances arising from the $n = 3$ levels were not included in the earlier work. For the same reason our present results may be underestimated for transitions with higher upper levels, because resonances arising from the $n = 4$ levels are not yet accounted for.

In Table 3 we list our values of Υ for transitions from the lowest 5 levels to higher excited levels over a wide electron temperature range of 10^5 to 10^7 K. These transitions are the most important and the temperature range included is suitable for applications in a wide variety of astrophysical, laser and fusion plasmas. The indices adopted to represent a transition have already been provided in Table 1. Our results of Υ for the remaining 820 transitions among the 46 fine-structure levels of Ca XV are presented in Table 4. We hope the presently reported results will be helpful in understanding plasma diagnostics.

4. Conclusions

Collision strengths among the lowest 46 fine-structure levels of Ca XV have been computed using the DARC code, and results of excitation rates in the form of effective collision strengths have been presented over a wide temperature range below 10^7 K. The present results are not only an extension of our earlier (solely available) *R*-matrix data (Aggarwal 1992), but also represent a significant overall improvement over those, due to (i) the adoption of larger range of partial waves, (ii) a wider energy range, and (iii) a better resolution of resonances in the entire threshold region. Yet there is scope for further improvements by including higher lying levels ($n = 4$), and extending the energy range beyond 300 Ryd. Both of these improvements can be a subject of further research.

We do not see any apparent deficiency in our calculations, but past experience shows that accuracy estimates can easily be in error. Nevertheless, our calculated values of Υ are expected

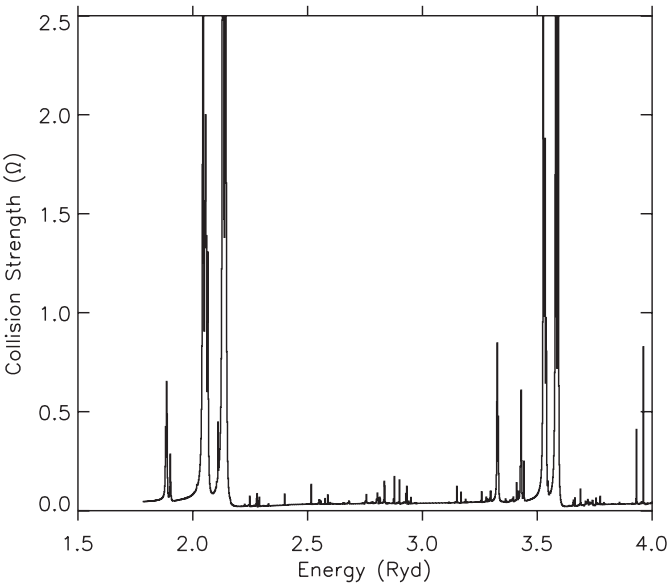

(a)

Fig. 3. Collision strengths (Ω) for the $(2s^2 2p^2)$ $^1D_2$–$^1S_0$ (4–5) transition of Ca XV. **a)** Results below 4 Ryd and **b)** results in entire threshold region up to 40 Ryd.

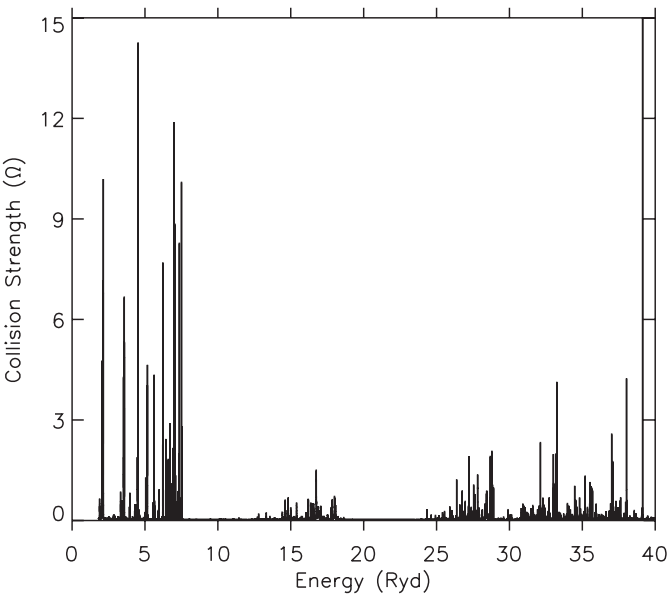

(b)

Fig. 3. Collision strengths (Ω) for the $(2s^2 2p^2)$ $^1D_2$–$^1S_0$ (4–5) transition of Ca XV. **a)** Results below 4 Ryd and **b)** results in entire threshold region up to 40 Ryd.

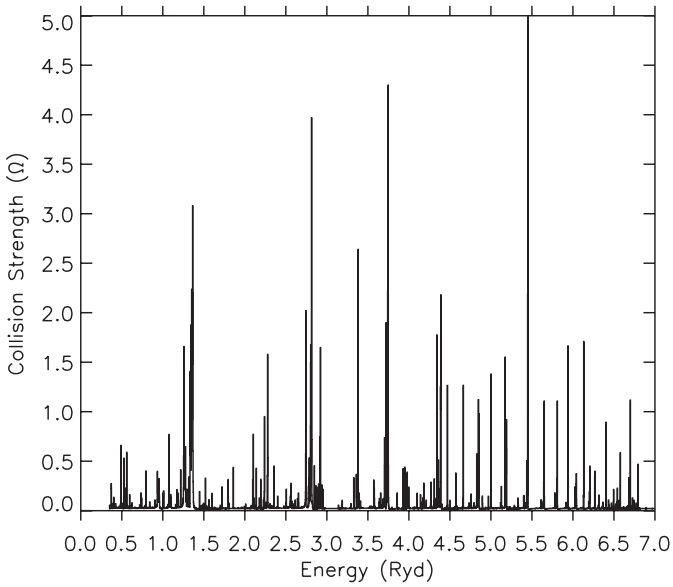

(a)

Fig. 4. Collision strengths (Ω) for the $(2s^2 2p^2)$ $^3P_0$–$^3P_2$ (1–3) transition of Ca XV. **a)** Results below 7 Ryd and **b)** results in entire threshold region up to 40 Ryd.

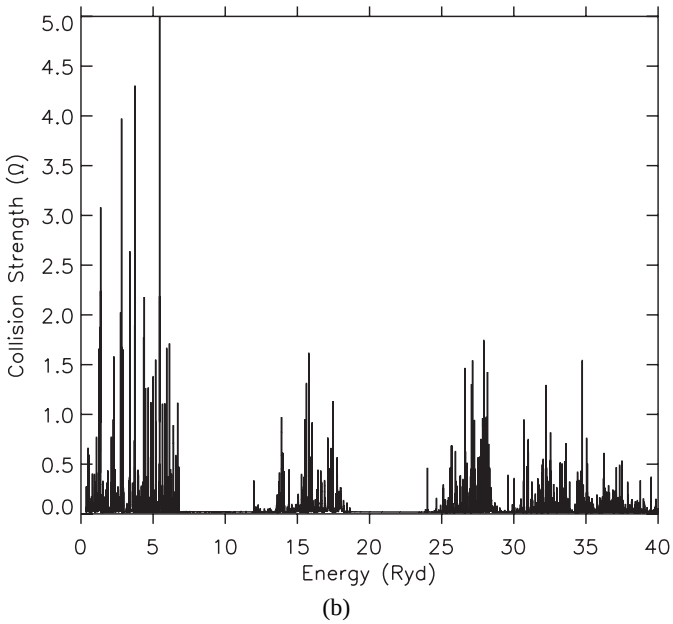

(b)

Fig. 4. Collision strengths (Ω) for the $(2s^2 2p^2)$ $^3P_0$–$^3P_2$ (1–3) transition of Ca XV. **a)** Results below 7 Ryd and **b)** results in entire threshold region up to 40 Ryd.

to be accurate to better than 20% for a majority of transitions, especially those with upper levels below 36, i.e. 2p3d $^3F^o_3$. This is because our calculations do not include resonances from the higher lying levels of $n = 4$. Similarly, results towards the lower end of the temperature range may have a comparatively lower accuracy because of the presence (or absence) of near threshold resonances. Additionally, this estimate is based on the presently adopted wavefunctions. As scope remains for improvement in our wavefunctions, the present values of Ω may significantly vary, especially for weaker transitions, and hence may affect the accuracy of our ϒ results. However, the corresponding values of ϒ for stronger transitions are unlikely to vary by more than 20%.

Acknowledgements. This work has been financed by the Engineering and Physical Sciences and Particle Physics and Astronomy Research Councils of the United Kingdom. A part of the computational work has been carried out on the MIRACLE Supercomputer at the HiPerSPACE Computer Centre at University College London, and we wish to thank Dr. Patrick Norrington for making his code available to us prior to publication.

Table 3. Effective collision strengths for transitions in Ca XV. ($a \pm b \equiv a \times 10^{\pm b}$).

Transition		Temperature (log K)										
I	J	5.00	5.20	5.40	5.60	5.80	6.00	6.20	6.40	6.60	6.80	7.00
1	2	2.387-1	2.253-1	2.055-1	1.805-1	1.525-1	1.258-1	1.031-1	8.389-2	6.691-2	5.179-2	3.885-2
1	3	6.914-2	7.398-2	7.490-2	7.173-2	6.535-2	5.799-2	5.113-2	4.479-2	3.863-2	3.284-2	2.780-2
1	4	4.855-2	4.349-2	3.834-2	3.318-2	2.874-2	2.573-2	2.378-2	2.180-2	1.906-2	1.570-2	1.225-2
1	5	8.017-3	7.869-3	7.321-3	6.512-3	5.845-3	5.628-3	5.693-3	5.603-3	5.083-3	4.210-3	3.231-3
1	6	2.562-2	2.405-2	2.113-2	1.759-2	1.419-2	1.133-2	9.070-3	7.312-3	5.903-3	4.728-3	3.718-3
1	7	1.188-2	1.035-2	8.866-3	7.580-3	6.537-3	5.707-3	5.020-3	4.407-3	3.816-3	3.225-3	2.641-3
1	8	2.167-1	2.167-1	2.173-1	2.190-1	2.222-1	2.277-1	2.357-1	2.471-1	2.629-1	2.837-1	3.074-1
1	9	1.102-2	8.428-3	6.189-3	4.394-3	3.043-3	2.074-3	1.402-3	9.429-4	6.314-4	4.205-4	2.787-4
1	10	6.553-4	5.995-4	5.400-4	4.830-4	4.334-4	3.910-4	3.526-4	3.143-4	2.740-4	2.318-4	1.893-4
1	11	1.025-1	1.029-1	1.034-1	1.042-1	1.057-1	1.082-1	1.118-1	1.170-1	1.243-1	1.338-1	1.447-1
1	12	2.178-3	2.063-3	1.874-3	1.666-3	1.477-3	1.314-3	1.171-3	1.034-3	8.967-4	7.567-4	6.178-4
1	13	1.003-1	1.007-1	1.013-1	1.022-1	1.036-1	1.058-1	1.090-1	1.137-1	1.203-1	1.289-1	1.387-1
1	14	2.257-3	2.216-3	2.171-3	2.125-3	2.076-3	2.011-3	1.913-3	1.773-3	1.589-3	1.372-3	1.137-3
1	15	6.011-4	6.032-4	6.026-4	6.029-4	6.026-4	5.951-4	5.750-4	5.396-4	4.907-4	4.333-4	3.733-4
1	16	1.031-3	1.040-3	1.074-3	1.129-3	1.172-3	1.184-3	1.158-3	1.100-3	1.022-3	9.395-4	8.624-4
1	17	6.625-5	1.142-4	2.137-4	3.457-4	4.548-4	5.125-4	5.170-4	4.707-4	3.890-4	2.967-4	2.131-4
1	18	4.880-4	5.506-4	6.580-4	7.884-4	8.928-4	9.603-4	9.889-4	9.571-4	8.641-4	7.386-4	6.105-4
1	19	1.118-4	1.460-4	2.272-4	3.383-4	4.266-4	4.678-4	4.624-4	4.158-4	3.428-4	2.630-4	1.913-4
1	20	2.062-4	2.930-4	4.099-4	5.149-4	5.626-4	5.575-4	5.159-4	4.443-4	3.551-4	2.663-4	1.904-4
1	21	7.455-3	6.595-3	5.386-3	4.146-3	3.069-3	2.226-3	1.603-3	1.156-3	8.369-4	6.056-4	4.358-4
1	22	4.213-2	3.874-2	3.238-2	2.516-2	1.864-2	1.347-2	9.750-3	7.258-3	5.738-3	4.966-3	4.738-3
1	23	1.432-2	1.164-2	8.948-3	6.548-3	4.618-3	3.181-3	2.165-3	1.466-3	9.931-4	6.730-4	4.557-4
1	24	2.298-2	1.800-2	1.362-2	9.862-3	6.891-3	4.698-3	3.162-3	2.124-3	1.440-3	9.986-4	7.208-4
1	25	3.798-2	3.265-2	2.568-2	1.913-2	1.384-2	9.922-3	7.133-3	5.169-3	3.774-3	2.761-3	2.010-3
1	26	1.120-2	9.737-3	8.180-3	6.772-3	5.645-3	4.815-3	4.241-3	3.869-3	3.659-3	3.584-3	3.596-3
1	27	7.587-2	5.784-2	4.157-2	2.887-2	1.971-2	1.340-2	9.137-3	6.285-3	4.361-3	3.044-3	2.126-3
1	28	3.289-3	2.844-3	2.324-3	1.839-3	1.439-3	1.132-3	8.981-4	7.172-4	5.713-4	4.494-4	3.462-4
1	29	1.014-1	6.526-2	4.194-2	2.693-2	1.732-2	1.117-2	7.236-3	4.718-3	3.095-3	2.042-3	1.352-3
1	30	3.895-2	3.658-2	3.385-2	3.136-2	2.940-2	2.805-2	2.726-2	2.692-2	2.696-2	2.726-2	2.756-2
1	31	3.809-3	3.329-3	2.799-3	2.315-3	1.918-3	1.603-3	1.351-3	1.140-3	9.517-4	7.791-4	6.207-4
1	32	6.079-3	5.077-3	4.065-3	3.201-3	2.532-3	2.037-3	1.675-3	1.406-3	1.199-3	1.038-3	9.092-4
1	33	3.592-3	2.923-3	2.327-3	1.845-3	1.478-3	1.202-3	9.911-4	8.202-4	6.743-4	5.454-4	4.314-4
1	34	9.570-3	8.248-3	7.191-3	6.366-3	5.696-3	5.104-3	4.527-3	3.932-3	3.314-3	2.696-3	2.110-3
1	35	5.738-4	4.767-4	3.946-4	3.304-4	2.819-4	2.450-4	2.153-4	1.898-4	1.664-4	1.447-4	1.247-4
1	36	6.267-3	5.582-3	5.088-3	4.732-3	4.467-3	4.261-3	4.093-3	3.960-3	3.870-3	3.833-3	3.831-3
1	37	9.163-3	8.294-3	7.650-3	7.132-3	6.657-3	6.161-3	5.603-3	4.964-3	4.254-3	3.511-3	2.784-3
1	38	1.220-3	1.171-3	1.125-3	1.078-3	1.024-3	9.589-4	8.775-4	7.792-4	6.673-4	5.491-4	4.335-4
1	39	7.472-2	7.523-2	7.593-2	7.693-2	7.850-2	8.104-2	8.512-2	9.143-2	1.006-1	1.131-1	1.283-1
1	40	2.506-3	2.460-3	2.403-3	2.329-3	2.228-3	2.093-3	1.919-3	1.705-3	1.461-3	1.203-3	9.504-4
1	41	1.628-3	1.599-3	1.567-3	1.527-3	1.476-3	1.411-3	1.327-3	1.228-3	1.118-3	1.007-3	9.008-4
1	42	7.299-4	7.022-4	6.751-4	6.463-4	6.128-4	5.716-4	5.208-4	4.604-4	3.927-4	3.221-4	2.538-4
1	43	1.145-3	1.126-3	1.109-3	1.093-3	1.076-3	1.058-3	1.040-3	1.026-3	1.019-3	1.028-3	1.052-3
1	44	3.238-4	3.151-4	3.064-4	2.966-4	2.844-4	2.685-4	2.480-4	2.226-4	1.931-4	1.612-4	1.291-4
1	45	1.395-3	1.389-3	1.382-3	1.370-3	1.354-3	1.334-3	1.313-3	1.297-3	1.293-3	1.311-3	1.351-3
1	46	1.847-3	1.826-3	1.793-3	1.744-3	1.671-3	1.571-3	1.439-3	1.275-3	1.089-3	8.919-4	7.004-4

Table 3. continued.

Transition		Temperature (log K)										
I	J	5.00	5.20	5.40	5.60	5.80	6.00	6.20	6.40	6.60	6.80	7.00
2	3	3.911-1	4.870-1	5.740-1	5.961-1	5.482-1	4.647-1	3.776-1	3.003-1	2.346-1	1.804-1	1.372-1
2	4	1.665-1	1.534-1	1.391-1	1.235-1	1.093-1	9.944-2	9.326-2	8.660-2	7.650-2	6.348-2	4.981-2
2	5	2.269-2	2.215-2	2.107-2	1.954-2	1.834-2	1.822-2	1.861-2	1.823-2	1.642-2	1.355-2	1.041-2
2	6	6.825-2	6.352-2	5.624-2	4.756-2	3.913-2	3.196-2	2.624-2	2.176-2	1.817-2	1.519-2	1.266-2
2	7	4.898-1	4.847-1	4.812-1	4.807-1	4.848-1	4.946-1	5.105-1	5.341-1	5.676-1	6.119-1	6.629-1
2	8	9.775-2	9.352-2	8.961-2	8.660-2	8.484-2	8.446-2	8.543-2	8.783-2	9.189-2	9.769-2	1.045-1
2	9	3.796-2	3.070-2	2.416-2	1.869-2	1.442-2	1.123-2	8.887-3	7.119-3	5.723-3	4.566-3	3.582-3
2	10	1.440-1	1.447-1	1.456-1	1.469-1	1.491-1	1.527-1	1.578-1	1.652-1	1.754-1	1.890-1	2.043-1
2	11	1.919-1	1.925-1	1.932-1	1.946-1	1.972-1	2.016-1	2.081-1	2.176-1	2.309-1	2.485-1	2.684-1
2	12	7.845-2	7.842-2	7.814-2	7.799-2	7.837-2	7.951-2	8.159-2	8.485-2	8.962-2	9.601-2	1.033-1
2	13	3.133-1	3.145-1	3.163-1	3.191-1	3.236-1	3.304-1	3.406-1	3.554-1	3.762-1	4.033-1	4.339-1
2	14	1.077-2	1.029-2	9.844-3	9.469-3	9.151-3	8.837-3	8.466-3	7.997-3	7.425-3	6.780-3	6.099-3
2	15	1.514-2	1.522-2	1.531-2	1.543-2	1.561-2	1.585-2	1.618-2	1.664-2	1.728-2	1.814-2	1.911-2
2	16	2.389-3	2.427-3	2.607-3	2.925-3	3.225-3	3.385-3	3.375-3	3.196-3	2.903-3	2.575-3	2.270-3
2	17	2.230-3	2.422-3	2.770-3	3.186-3	3.500-3	3.663-3	3.676-3	3.505-3	3.170-3	2.759-3	2.353-3
2	18	1.002-4	1.563-4	2.669-4	4.088-4	5.221-4	5.771-4	5.738-4	5.174-4	4.258-4	3.248-4	2.342-4
2	19	4.633-4	5.716-4	8.353-4	1.203-3	1.501-3	1.652-3	1.654-3	1.514-3	1.271-3	9.947-4	7.392-4
2	20	4.718-4	6.985-4	1.046-3	1.394-3	1.576-3	1.583-3	1.461-3	1.244-3	9.799-4	7.234-4	5.084-4
2	21	3.310-2	2.854-2	2.285-2	1.730-2	1.266-2	9.157-3	6.725-3	5.181-3	4.338-3	4.051-3	4.177-3
2	22	8.352-2	6.976-2	5.460-2	4.061-2	2.919-2	2.062-2	1.455-2	1.042-2	7.716-3	6.026-3	5.047-3
2	23	2.609-1	2.020-1	1.477-1	1.037-1	7.100-2	4.792-2	3.231-2	2.208-2	1.561-2	1.173-2	9.610-3
2	24	1.505-1	1.077-1	7.539-2	5.170-2	3.487-2	2.328-2	1.548-2	1.032-2	6.943-3	4.740-3	3.313-3
2	25	3.854-2	3.286-2	2.626-2	2.019-2	1.532-2	1.170-2	9.110-3	7.291-3	6.018-3	5.131-3	4.507-3
2	26	4.047-2	3.342-2	2.657-2	2.064-2	1.594-2	1.240-2	9.790-3	7.847-3	6.359-3	5.189-3	4.252-3
2	27	8.378-2	6.687-2	5.126-2	3.864-2	2.925-2	2.263-2	1.813-2	1.512-2	1.316-2	1.189-2	1.105-2
2	28	2.255-2	1.960-2	1.630-2	1.323-2	1.072-2	8.830-3	7.459-3	6.492-3	5.828-3	5.399-3	5.132-3
2	29	9.711-2	7.136-2	5.232-2	3.851-2	2.879-2	2.217-2	1.775-2	1.485-2	1.299-2	1.180-2	1.099-2
2	30	7.330-3	6.350-3	5.325-3	4.402-3	3.646-3	3.049-3	2.569-3	2.165-3	1.805-3	1.474-3	1.172-3
2	31	9.221-2	8.587-2	7.964-2	7.436-2	7.043-2	6.784-2	6.642-2	6.595-2	6.623-2	6.706-2	6.779-2
2	32	2.516-2	2.138-2	1.743-2	1.395-2	1.118-2	9.084-3	7.510-3	6.300-3	5.335-3	4.546-3	3.888-3
2	33	1.825-2	1.503-2	1.205-2	9.605-3	7.721-3	6.304-3	5.218-3	4.347-3	3.608-3	2.962-3	2.394-3
2	34	1.647-2	1.432-2	1.266-2	1.140-2	1.043-2	9.640-3	8.943-3	8.302-3	7.718-3	7.222-3	6.816-3
2	35	1.905-3	1.599-3	1.342-3	1.139-3	9.807-4	8.535-4	7.432-4	6.396-4	5.382-4	4.389-4	3.452-4
2	36	1.651-2	1.476-2	1.335-2	1.220-2	1.121-2	1.026-2	9.280-3	8.222-3	7.103-3	5.976-3	4.909-3
2	37	5.645-2	5.495-2	5.396-2	5.343-2	5.336-2	5.385-2	5.515-2	5.757-2	6.145-2	6.714-2	7.430-2
2	38	1.259-2	1.083-2	9.517-3	8.551-3	7.822-3	7.234-3	6.723-3	6.259-3	5.840-3	5.485-3	5.187-3
2	39	2.822-2	2.771-2	2.736-2	2.713-2	2.702-2	2.706-2	2.736-2	2.806-2	2.933-2	3.136-2	3.404-2
2	40	1.018-1	1.021-1	1.027-1	1.039-1	1.058-1	1.090-1	1.144-1	1.227-1	1.347-1	1.513-1	1.714-1
2	41	1.196-2	1.126-2	1.071-2	1.023-2	9.749-3	9.203-3	8.560-3	7.812-3	6.984-3	6.132-3	5.307-3
2	42	1.808-2	1.806-2	1.804-2	1.805-2	1.811-2	1.827-2	1.861-2	1.926-2	2.034-2	2.198-2	2.410-2
2	43	3.998-2	4.025-2	4.060-2	4.109-2	4.187-2	4.312-2	4.514-2	4.826-2	5.279-2	5.906-2	6.668-2
2	44	1.900-2	1.915-2	1.933-2	1.960-2	2.000-2	2.065-2	2.166-2	2.321-2	2.545-2	2.853-2	3.226-2
2	45	4.641-3	4.599-3	4.534-3	4.437-3	4.296-3	4.102-3	3.853-3	3.554-3	3.227-3	2.904-3	2.614-3
2	46	7.779-3	7.693-3	7.557-3	7.353-3	7.055-3	6.640-3	6.094-3	5.418-3	4.645-3	3.830-3	3.036-3

Table 3. continued.

Transition		Temperature (log K)										
I	J	5.00	5.20	5.40	5.60	5.80	6.00	6.20	6.40	6.60	6.80	7.00
3	4	3.926-1	3.731-1	3.488-1	3.146-1	2.769-1	2.455-1	2.217-1	1.986-1	1.712-1	1.404-1	1.102-1
3	5	2.339-2	2.383-2	2.345-2	2.245-2	2.188-2	2.262-2	2.388-2	2.395-2	2.201-2	1.855-2	1.462-2
3	6	9.901-2	9.524-2	8.593-2	7.355-2	6.103-2	5.019-2	4.150-2	3.467-2	2.923-2	2.477-2	2.104-2
3	7	8.138-2	7.076-2	6.065-2	5.193-2	4.511-2	4.024-2	3.704-2	3.521-2	3.451-2	3.476-2	3.564-2
3	8	3.126-2	2.599-2	2.071-2	1.583-2	1.173-2	8.558-3	6.259-3	4.666-3	3.602-3	2.922-3	2.507-3
3	9	7.102-1	6.922-1	6.793-1	6.727-1	6.741-1	6.844-1	7.036-1	7.333-1	7.765-1	8.347-1	9.021-1
3	10	3.638-3	3.622-3	3.358-3	2.964-3	2.559-3	2.202-3	1.898-3	1.632-3	1.386-3	1.152-3	9.302-4
3	11	1.401-1	1.401-1	1.400-1	1.403-1	1.415-1	1.440-1	1.481-1	1.542-1	1.631-1	1.750-1	1.886-1
3	12	6.457-1	6.476-1	6.503-1	6.553-1	6.646-1	6.799-1	7.026-1	7.352-1	7.808-1	8.409-1	9.091-1
3	13	6.406-1	6.432-1	6.471-1	6.533-1	6.631-1	6.777-1	6.993-1	7.303-1	7.735-1	8.303-1	8.941-1
3	14	5.165-2	5.149-2	5.138-2	5.139-2	5.156-2	5.194-2	5.255-2	5.350-2	5.493-2	5.696-2	5.930-2
3	15	6.967-3	6.955-3	6.899-3	6.808-3	6.678-3	6.478-3	6.172-3	5.730-3	5.146-3	4.450-3	3.694-3
3	16	4.436-3	4.693-3	5.353-3	6.333-3	7.218-3	7.774-3	7.941-3	7.628-3	6.890-3	5.952-3	5.022-3
3	17	2.206-3	2.271-3	2.477-3	2.803-3	3.090-3	3.231-3	3.207-3	3.028-3	2.744-3	2.433-3	2.148-3
3	18	9.729-4	9.875-4	1.036-3	1.103-3	1.151-3	1.161-3	1.134-3	1.074-3	9.935-4	9.121-4	8.387-4
3	19	1.347-3	1.627-3	2.141-3	2.782-3	3.272-3	3.489-3	3.438-3	3.134-3	2.652-3	2.117-3	1.624-3
3	20	3.304-4	6.040-4	1.066-3	1.554-3	1.846-3	1.910-3	1.797-3	1.551-3	1.236-3	9.224-4	6.553-4
3	21	1.816-2	1.496-2	1.174-2	8.810-3	6.399-3	4.565-3	3.236-3	2.298-3	1.637-3	1.168-3	8.300-4
3	22	1.133-1	9.390-2	7.337-2	5.451-2	3.912-2	2.759-2	1.949-2	1.411-2	1.075-2	8.886-3	8.077-3
3	23	3.329-1	2.806-1	2.184-1	1.606-1	1.138-1	7.917-2	5.503-2	3.905-2	2.907-2	2.345-2	2.086-2
3	24	1.142-1	8.472-2	6.140-2	4.350-2	3.032-2	2.097-2	1.451-2	1.009-2	7.064-3	4.966-3	3.488-3
3	25	3.132-2	2.583-2	2.057-2	1.603-2	1.244-2	9.760-3	7.803-3	6.373-3	5.310-3	4.509-3	3.893-3
3	26	5.979-2	5.035-2	4.078-2	3.249-2	2.602-2	2.128-2	1.795-2	1.563-2	1.405-2	1.299-2	1.226-2
3	27	2.604-2	2.193-2	1.771-2	1.394-2	1.091-2	8.586-3	6.830-3	5.472-3	4.376-3	3.461-3	2.685-3
3	28	8.453-2	7.037-2	5.605-2	4.347-2	3.352-2	2.616-2	2.090-2	1.721-2	1.464-2	1.288-2	1.169-2
3	29	2.676-2	2.316-2	1.899-2	1.506-2	1.180-2	9.275-3	7.357-3	5.876-3	4.692-3	3.715-3	2.895-3
3	30	5.208-3	4.442-3	3.719-3	3.110-3	2.634-3	2.279-3	2.016-3	1.821-3	1.677-3	1.576-3	1.505-3
3	31	3.538-2	2.942-2	2.354-2	1.844-2	1.440-2	1.138-2	9.160-3	7.523-3	6.286-3	5.333-3	4.584-3
3	32	2.224-1	2.016-1	1.813-1	1.642-1	1.514-1	1.429-1	1.377-1	1.352-1	1.346-1	1.354-1	1.361-1
3	33	3.441-2	2.961-2	2.481-2	2.065-2	1.734-2	1.477-2	1.274-2	1.106-2	9.601-3	8.296-3	7.121-3
3	34	2.441-2	2.161-2	1.946-2	1.783-2	1.658-2	1.558-2	1.473-2	1.400-2	1.343-2	1.307-2	1.293-2
3	35	3.378-3	2.830-3	2.382-3	2.034-3	1.764-3	1.547-3	1.355-3	1.174-3	9.954-4	8.203-4	6.554-4
3	36	4.771-2	4.395-2	4.105-2	3.898-2	3.764-2	3.692-2	3.684-2	3.751-2	3.906-2	4.172-2	4.526-2
3	37	2.315-2	2.097-2	1.931-2	1.804-2	1.704-2	1.618-2	1.542-2	1.474-2	1.419-2	1.386-2	1.376-2
3	38	3.043-2	2.624-2	2.303-2	2.062-2	1.873-2	1.712-2	1.565-2	1.423-2	1.287-2	1.161-2	1.049-2
3	39	7.773-3	7.080-3	6.560-3	6.161-3	5.831-3	5.529-3	5.229-3	4.924-3	4.630-3	4.370-3	4.150-3
3	40	2.282-2	2.120-2	1.994-2	1.887-2	1.785-2	1.676-2	1.552-2	1.410-2	1.254-2	1.096-2	9.445-3
3	41	2.393-1	2.407-1	2.422-1	2.444-1	2.479-1	2.541-1	2.649-1	2.822-1	3.080-1	3.440-1	3.881-1
3	42	1.108-1	1.116-1	1.124-1	1.135-1	1.153-1	1.182-1	1.231-1	1.308-1	1.423-1	1.583-1	1.778-1
3	43	3.114-2	3.125-2	3.138-2	3.156-2	3.187-2	3.240-2	3.333-2	3.491-2	3.734-2	4.087-2	4.529-2
3	44	2.038-3	1.994-3	1.943-3	1.876-3	1.789-3	1.672-3	1.523-3	1.343-3	1.140-3	9.293-4	7.267-4
3	45	7.713-3	7.627-3	7.491-3	7.285-3	6.986-3	6.570-3	6.024-3	5.351-3	4.583-3	3.773-3	2.985-3
3	46	1.778-2	1.761-2	1.735-2	1.695-2	1.639-2	1.562-2	1.462-2	1.343-2	1.211-2	1.081-2	9.626-3

Table 3. continued.

Transition		Temperature (log K)										
I	J	5.00	5.20	5.40	5.60	5.80	6.00	6.20	6.40	6.60	6.80	7.00
4	5	2.023-1	1.787-1	1.588-1	1.406-1	1.223-1	1.052-1	9.111-2	8.012-2	7.134-2	6.438-2	5.912-2
4	6	2.075-2	2.065-2	1.892-2	1.579-2	1.221-2	8.975-3	6.412-3	4.530-3	3.202-3	2.278-3	1.636-3
4	7	5.549-2	5.417-2	5.022-2	4.473-2	3.903-2	3.394-2	2.964-2	2.599-2	2.277-2	1.982-2	1.710-2
4	8	3.531-2	3.425-2	3.181-2	2.858-2	2.530-2	2.239-2	1.994-2	1.783-2	1.595-2	1.423-2	1.264-2
4	9	1.117-1	1.094-1	1.031-1	9.480-2	8.658-2	7.975-2	7.462-2	7.106-2	6.890-2	6.801-2	6.802-2
4	10	6.012-3	5.581-3	4.846-3	4.005-3	3.228-3	2.590-3	2.091-3	1.699-3	1.378-3	1.105-3	8.674-4
4	11	2.999-2	2.770-2	2.461-2	2.142-2	1.866-2	1.651-2	1.496-2	1.388-2	1.318-2	1.278-2	1.258-2
4	12	4.648-2	4.324-2	3.846-2	3.330-2	2.868-2	2.494-2	2.200-2	1.966-2	1.772-2	1.607-2	1.464-2
4	13	1.296-2	1.031-2	7.840-3	5.845-3	4.372-3	3.331-3	2.597-3	2.063-3	1.662-3	1.356-3	1.124-3
4	14	1.348-0	1.341-0	1.337-0	1.342-0	1.355-0	1.382-0	1.424-0	1.487-0	1.577-0	1.696-0	1.829-0
4	15	6.840-1	6.877-1	6.929-1	7.005-1	7.115-1	7.277-1	7.513-1	7.851-1	8.323-1	8.941-1	9.635-1
4	16	1.315-3	1.381-3	1.687-3	2.246-3	2.810-3	3.161-3	3.232-3	3.014-3	2.585-3	2.076-3	1.596-3
4	17	7.079-4	7.188-4	8.323-4	1.054-3	1.275-3	1.408-3	1.424-3	1.321-3	1.131-3	9.079-4	6.972-4
4	18	1.995-4	2.000-4	2.282-4	2.848-4	3.403-4	3.707-4	3.692-4	3.371-4	2.842-4	2.244-4	1.685-4
4	19	8.498-3	9.010-3	9.935-3	1.102-2	1.177-2	1.203-2	1.186-2	1.124-2	1.028-2	9.211-3	8.203-3
4	20	1.636-3	1.928-3	2.329-3	2.659-3	2.793-3	2.802-3	2.745-3	2.578-3	2.289-3	1.938-3	1.597-3
4	21	2.090-2	1.776-2	1.416-2	1.068-2	7.721-3	5.437-3	3.777-3	2.612-3	1.806-3	1.250-3	8.631-4
4	22	1.279-1	1.090-1	8.514-2	6.252-2	4.404-2	3.026-2	2.055-2	1.396-2	9.590-3	6.753-3	4.951-3
4	23	2.042-1	1.625-1	1.229-1	8.927-2	6.306-2	4.387-2	3.039-2	2.114-2	1.485-2	1.056-2	7.645-3
4	24	4.404-0	2.926-0	1.919-0	1.247-0	8.041-1	5.164-1	3.313-1	2.134-1	1.390-1	9.275-2	6.469-2
4	25	1.900-1	1.622-1	1.252-1	9.056-2	6.305-2	4.305-2	2.923-2	1.998-2	1.389-2	9.933-3	7.378-3
4	26	6.149-2	5.269-2	4.253-2	3.314-2	2.553-2	1.977-2	1.553-2	1.241-2	1.005-2	8.207-3	6.728-3
4	27	4.531-1	3.433-1	2.446-1	1.679-1	1.127-1	7.496-2	4.985-2	3.346-2	2.288-2	1.613-2	1.186-2
4	28	6.432-2	5.416-2	4.439-2	3.582-2	2.885-2	2.343-2	1.920-2	1.578-2	1.291-2	1.041-2	8.235-3
4	29	6.178-1	3.979-1	2.562-1	1.652-1	1.069-1	6.970-2	4.590-2	3.068-2	2.091-2	1.461-2	1.053-2
4	30	9.442-3	6.921-3	5.076-3	3.750-3	2.815-3	2.158-3	1.689-3	1.340-3	1.067-3	8.443-4	6.588-4
4	31	2.269-2	1.905-2	1.550-2	1.244-2	1.000-2	8.130-3	6.682-3	5.514-3	4.526-3	3.663-3	2.905-3
4	32	4.652-2	3.937-2	3.232-2	2.610-2	2.109-2	1.724-2	1.433-2	1.209-2	1.030-2	8.829-3	7.595-3
4	33	2.675-1	2.530-1	2.298-1	2.048-1	1.833-1	1.674-1	1.568-1	1.506-1	1.479-1	1.475-1	1.479-1
4	34	3.021-2	2.755-2	2.533-2	2.358-2	2.228-2	2.135-2	2.077-2	2.054-2	2.073-2	2.143-2	2.256-2
4	35	5.509-3	4.841-3	4.182-3	3.624-3	3.208-3	2.934-3	2.787-3	2.754-3	2.828-3	3.000-3	3.230-3
4	36	3.544-2	3.152-2	2.809-2	2.529-2	2.300-2	2.106-2	1.929-2	1.759-2	1.597-2	1.450-2	1.326-2
4	37	4.738-2	4.547-2	4.400-2	4.304-2	4.261-2	4.281-2	4.381-2	4.585-2	4.917-2	5.402-2	6.005-2
4	38	5.055-2	4.521-2	4.046-2	3.646-2	3.302-2	2.984-2	2.667-2	2.333-2	1.983-2	1.629-2	1.290-2
4	39	9.407-3	8.122-3	7.087-3	6.269-3	5.604-3	5.023-3	4.468-3	3.908-3	3.338-3	2.779-3	2.257-3
4	40	3.155-2	3.002-2	2.870-2	2.766-2	2.688-2	2.637-2	2.614-2	2.628-2	2.691-2	2.819-2	3.000-2
4	41	3.093-2	2.809-2	2.559-2	2.348-2	2.164-2	1.990-2	1.814-2	1.627-2	1.433-2	1.242-2	1.066-2
4	42	3.002-2	2.867-2	2.755-2	2.664-2	2.588-2	2.523-2	2.471-2	2.439-2	2.440-2	2.489-2	2.586-2
4	43	1.131-2	1.065-2	1.008-2	9.574-3	9.083-3	8.559-3	7.973-3	7.322-3	6.635-3	5.971-3	5.379-3
4	44	3.134-3	2.940-3	2.773-3	2.620-3	2.463-3	2.286-3	2.077-3	1.834-3	1.562-3	1.279-3	1.005-3
4	45	7.903-3	7.913-3	7.936-3	7.978-3	8.052-3	8.178-3	8.394-3	8.746-3	9.282-3	1.004-2	1.094-2
4	46	3.168-1	3.173-1	3.184-1	3.206-1	3.253-1	3.342-1	3.499-1	3.753-1	4.128-1	4.648-1	5.283-1

Table 3. continued.

Transition		Temperature (log K)										
I	J	5.00	5.20	5.40	5.60	5.80	6.00	6.20	6.40	6.60	6.80	7.00
5	6	1.358-3	1.439-3	1.363-3	1.157-3	8.988-4	6.565-4	4.610-4	3.161-4	2.138-4	1.435-4	9.573-5
5	7	3.990-3	3.609-3	3.046-3	2.414-3	1.824-3	1.340-3	9.723-4	7.036-4	5.086-4	3.662-4	2.617-4
5	8	5.537-3	5.197-3	4.764-3	4.332-3	3.979-3	3.744-3	3.627-3	3.621-3	3.731-3	3.954-3	4.259-3
5	9	4.794-3	4.302-3	3.604-3	2.820-3	2.084-3	1.480-3	1.025-3	6.991-4	4.709-4	3.133-4	2.061-4
5	10	3.944-3	3.786-3	3.559-3	3.302-3	3.048-3	2.808-3	2.574-3	2.329-3	2.062-3	1.771-3	1.467-3
5	11	1.603-2	1.546-2	1.467-2	1.381-2	1.301-2	1.234-2	1.177-2	1.127-2	1.083-2	1.046-2	1.013-2
5	12	1.717-2	1.631-2	1.509-2	1.370-2	1.235-2	1.113-2	1.002-2	8.936-3	7.825-3	6.666-3	5.485-3
5	13	7.705-3	6.944-3	6.283-3	5.788-3	5.466-3	5.299-3	5.264-3	5.352-3	5.561-3	5.887-3	6.282-3
5	14	3.910-2	2.863-2	2.007-2	1.370-2	9.228-3	6.190-3	4.167-3	2.828-3	1.938-3	1.339-3	9.306-4
5	15	2.599-1	2.612-1	2.629-1	2.656-1	2.697-1	2.758-1	2.849-1	2.980-1	3.162-1	3.399-1	3.665-1
5	16	1.653-4	1.661-4	1.928-4	2.616-4	3.420-4	3.973-4	4.121-4	3.833-4	3.226-4	2.504-4	1.830-4
5	17	1.704-4	1.704-4	1.951-4	2.490-4	3.039-4	3.347-4	3.343-4	3.038-4	2.530-4	1.960-4	1.438-4
5	18	7.644-5	7.618-5	8.569-5	1.050-4	1.235-4	1.330-4	1.317-4	1.199-4	1.011-4	8.017-5	6.081-5
5	19	7.041-4	7.135-4	7.653-4	8.483-4	9.150-4	9.451-4	9.419-4	9.049-4	8.413-4	7.693-4	7.026-4
5	20	2.571-3	3.010-3	3.391-3	3.621-3	3.681-3	3.712-3	3.749-3	3.636-3	3.300-3	2.824-3	2.331-3
5	21	3.370-3	2.789-3	2.181-3	1.624-3	1.166-3	8.189-4	5.696-4	3.956-4	2.755-4	1.922-4	1.340-4
5	22	4.749-2	4.256-2	3.535-2	2.725-2	1.978-2	1.376-2	9.317-3	6.221-3	4.140-3	2.776-3	1.900-3
5	23	4.372-2	3.489-2	2.656-2	1.939-2	1.374-2	9.561-3	6.608-3	4.569-3	3.170-3	2.206-3	1.534-3
5	24	2.055-0	1.741-0	1.393-0	1.042-0	7.382-1	5.029-1	3.339-1	2.183-1	1.416-1	9.196-2	6.035-2
5	25	5.527-0	4.728-0	3.616-0	2.576-0	1.755-0	1.162-0	7.561-1	4.865-1	3.108-1	1.977-1	1.254-1
5	26	4.207-2	3.254-2	2.368-2	1.661-2	1.144-2	7.838-3	5.388-3	3.733-3	2.608-3	1.831-3	1.285-3
5	27	1.497+1	1.123+1	7.909-0	5.347-0	3.524-0	2.286-0	1.468-0	9.366-1	5.952-1	3.773-1	2.388-1
5	28	1.359-2	1.167-2	9.579-3	7.670-3	6.109-3	4.898-3	3.962-3	3.216-3	2.596-3	2.062-3	1.600-3
5	29	2.133+1	1.354+1	8.580-0	5.428-0	3.431-0	2.168-0	1.369-0	8.646-1	5.461-1	3.449-1	2.178-1
5	30	1.693-1	1.076-1	6.831-2	4.331-2	2.746-2	1.741-2	1.106-2	7.037-3	4.491-3	2.878-3	1.855-3
5	31	6.726-3	5.795-3	4.730-3	3.742-3	2.932-3	2.308-3	1.835-3	1.468-3	1.171-3	9.223-4	7.115-4
5	32	1.218-2	9.593-3	7.302-3	5.463-3	4.086-3	3.094-3	2.387-3	1.877-3	1.498-3	1.211-3	9.880-4
5	33	1.071-2	8.832-3	7.116-3	5.713-3	4.671-3	3.961-3	3.524-3	3.305-3	3.263-3	3.367-3	3.560-3
5	34	2.626-3	2.239-3	1.905-3	1.634-3	1.416-3	1.234-3	1.072-3	9.158-4	7.630-4	6.154-4	4.787-4
5	35	4.092-2	3.742-2	3.420-2	3.161-2	2.976-2	2.857-2	2.793-2	2.773-2	2.789-2	2.830-2	2.870-2
5	36	4.091-3	3.604-3	3.182-3	2.834-3	2.542-3	2.280-3	2.023-3	1.758-3	1.484-3	1.208-3	9.461-4
5	37	3.363-3	2.873-3	2.427-3	2.059-3	1.763-3	1.518-3	1.302-3	1.100-3	9.070-4	7.244-4	5.587-4
5	38	7.455-3	6.757-3	6.167-3	5.671-3	5.226-3	4.787-3	4.314-3	3.790-3	3.221-3	2.636-3	2.072-3
5	39	2.086-3	1.827-3	1.630-3	1.484-3	1.375-3	1.292-3	1.227-3	1.180-3	1.154-3	1.154-3	1.181-3
5	40	3.721-3	3.321-3	2.983-3	2.702-3	2.457-3	2.224-3	1.984-3	1.727-3	1.456-3	1.182-3	9.226-4
5	41	3.639-3	3.240-3	2.924-3	2.666-3	2.437-3	2.210-3	1.968-3	1.706-3	1.428-3	1.149-3	8.897-4
5	42	5.581-3	5.209-3	4.899-3	4.623-3	4.346-3	4.040-3	3.681-3	3.262-3	2.793-3	2.300-3	1.819-3
5	43	4.556-3	4.241-3	3.990-3	3.773-3	3.560-3	3.327-3	3.056-3	2.742-3	2.391-3	2.026-3	1.672-3
5	44	1.790-3	1.656-3	1.552-3	1.464-3	1.378-3	1.284-3	1.174-3	1.044-3	8.988-4	7.446-4	5.924-4
5	45	7.637-2	7.668-2	7.719-2	7.805-2	7.955-2	8.213-2	8.641-2	9.307-2	1.027-1	1.159-1	1.319-1
5	46	2.355-3	2.364-3	2.378-3	2.400-3	2.437-3	2.496-3	2.590-3	2.732-3	2.933-3	3.194-3	3.477-3

References

Aggarwal, K. M. 1992, ApJS, 80, 453

Aggarwal, K. M., Hibbert, A., Keenan, F. P., & Norrington, P. H. 1997, ApJS, 108, 575

Aggarwal, K. M., & Keenan, F. P. 2002, Phys. Scr., 65, 383

Bhatia, A. K., & Doschek, G. A. 1993, At. Data Nucl. Data Tables, 53, 195

Dyall, K. G., Grant, I. P., Johnson, C. T., Parpia, F. A., & Plummer, E. P. 1989, Comput. Phys. Comm., 55, 424

Keenan, F. P., Conlon, E. S., Foster, V. J., Aggarwal, K. M., & Widing, K. G. 1992, ApJ, 401, 411

Mazzotta, P., Mazzitelli, G., Colafrancesco, S., & Vittorio, N. 1998, A&AS, 133, 403

Norrington, P. H., & Grant, I. P. 2003, Comput. Phys. Comm., in preparation

Sugar, J., & Corliss, C. 1985, J. Phys. Chem. Ref. Data Suppl., 14, 97

Zhang, H. L., & Sampson, D. H. 1996, At. Data Nucl. Data Tables, 63, 275